International Journal of Heat and Mass Transfer 52 (2009) 4125–4133

Contents lists available at ScienceDirect

International Journal of Heat and Mass Transfer

journal homepage: www.elsevier.com/locate/ijhmt

Discrete reaction model for composition of sooting flames

S.V. Zhubrin *

Flowsolve Ltd., Middle Floor, 40 High Street, Wimbledon Village, London SW19 5AU, United Kingdom

ARTICLE INFO

Article history:
Received 9 January 2009
Accepted 23 March 2009
Available online 18 May 2009

Keywords:
Soot formation
Combustion
Element balances
Mixture fraction

ABSTRACT

A discrete reaction model of sooting combustion is proposed on the grounds of multi-stage representation of oxidation chemistry. It is demonstrated that the predictions are in fair agreement to the measured data, and show the correct trends with no adjustments to the soot modelling concept. The practical applications of the model are also presented. The algebraic nature of the model relationships makes it easy to bring them into the computational loops of available predictive tools, so that it is believed the present model has the potential to supplant or complement the similar methods in the engineering computational analysis of combustion.

1. Introduction

Calculating the composition of sooting flames presents a challenging problem. It is currently solved by a number of demanding and sophisticated numerical techniques. The simplest of them uses empirically based correlations. Thus, it has a very limited range of applicability [1]. At the other end, the most popular research methods employ a family of the conservation equations along with PDF, probability density functions, in an attempt to address the detailed stochastic mechanism of soot formation and oxidation [2]. The resulting computing and intellectual requirements may far exceed what is generally available to the combustion and fire safety engineering communities. We shall refer to such methods as the "detailed approaches" in the reminder of the text.

The engineering practice, however, is in permanent need of affordable, easy for use, and reasonably accurate modelling tool to handle the diversity of the combustion problems arising from soot-forming under-ventilated environment, and/or fuel-enriched operating conditions of many real-life fires and flames.

In a response to this demand, some authors [3,4] have attempted to find the reaction-model-based alternative to the detailed methods of soot-forming combustion. They have argued [3] that the sooting effects of combustion may be modelled using an extended form of chemical reaction for complete combustion. Their model uses the soot conversion factor, which is defined as a fraction of carbon, originally presented in the fuel that is converted to the soot during combustion. It is then assumed that the factor is a constant specific to the particular fuel. As a consequence, the soot content by mass becomes proportional to the total product mass fraction which is, in turn, made related to the local value of mixture fraction by the fast reaction approximation. The success of the method depends crucially on the value of the soot conversion factor; with the latter being empirically increased by more than one order of magnitude for heavily sooting fuels to get agreement with experimental observations.

A recent attempt [4] to design more realistically simplified reaction model has lead to bringing into the picture the carbon monoxide as another product of incomplete oxidation. The calculation procedure has then required two conversion factors, governing the rates of molar production for both the soot and carbon monoxide. The factors have been computed by making them proportional to the molar production of carbon dioxide. Using the fast reactions assumption the mixture fraction concept has again been employed. This model also makes use of experimental data to adjust the proportionality coefficients of conversion factors to predict the quantities of interest.

While practically attractive because of their simplicity, both foregoing types of analysis are not recommended by the present writer for a number of reasons: (i) the conversion factors are usually a function of local mixture composition, and not constant; (ii) for the simulation to be reliable, its conditions must be close to those of experiments; and (iii) the types of fuel and oxidizer should be similar to the ones on which the calibration was based. These methods will be referred to as the "simplified approaches" in the reminder of the text.

The purpose of this paper is to provide the reader with reasonably a simple yet realistic and comprehensive method by which he or she may mathematically predict the composition of flames with special emphasis on sooting effects.

* Tel.: +44 02083362086.
E-mail address: svzhubrin@yahoo.co.uk

0017-9310/$ - see front matter © 2009 Elsevier Ltd. All rights reserved.
doi:10.1016/j.ijheatmasstransfer.2009.03.034

Nomenclature

a	absorption coefficient (1/m)
C_g	symmetry factor of a scattering phase function
f	mixture fraction
i	i-species
L	distance function (m)
m	mass fraction (kg/kg)
s	scattering coefficient (1/m)
S	source term
T	temperature (K)
$\vec{V}$	velocity vector (m/s)
W_{gap}	distance between adjacent walls (m)
x	number of C-atoms in fuel molecule
y	number of H-atoms in fuel molecule

Greek symbols

Γ	exchange coefficient (kg/(m s))
Γ_R	radiative exchange coefficient (m)
ϕ	equivalence ratio
φ	general conserved scalar
ρ	density (kg/m^3)
χ	stoichiometric air-to fuel ratio

Subscripts

CO	carbon monoxide
CO_2	carbon dioxide
$C_{(S)}$	carbon soot
fu	C_xH_y-fuel
H_2O	water
i	i-species
in	intermediate
N_2	nitrogen
O_2	oxygen
s	sooting
st	stoichiometric
(α)	α-element

2. Foundation

The theoretical foundation for the present text follows the approach based on the mass fractions of mixture components as well as on the one that based on the mass fractions of elements [5]. A justification for the use of these, widely adapted mixture characteristics, is that, historically, the former is well rooted in the engineering practice, while the latter successfully exploits the fact that in the chemical reactions the elements are individually conserved, and, thus, their respective mass fractions can be most easily calculated from the balance equations which do not require any specific sources/sinks.

Component-based and element-based approaches are easily inter-converted as follows [6],

$$m_{(\alpha)} = \sum_i m_{(\alpha)i} m_i, \tag{1}$$

where $m_{(\alpha)}$ is the mass fraction of chemical element (α); m_i is the mass fraction of species i; $m_{(\alpha)i}$ is an (α)-element mass fraction in species i, which can be obtained from the chemical formula for i and atomic weights. For the element mass fractions known from their balance equations, inter-conversion equations can be viewed as a set of "number of element" – equations in "number of component" – unknowns.

The purpose of this paper is to reduce the product composition problem to the form of closed sets of inter-conversion equations, and then solve them for the mass fraction of product components with associated limiting requirements.

3. Description of the model

The useful solutions for the product composition are obtained here by (a) discretization of oxidation chemistry followed by (b) the restrictions on the number of product species involved, and (c) the assumption of fast reaction rates.

3.1. Discrete chemical reactions

It is assumed that oxidation of the hydrocarbon fuel in the presence of oxygen from atmospheric air proceeds in four reaction stages, namely:

1. To create CO_2 and H_2O when the air is in excess in accord with the following chemical equation:

$$C_xH_y + \frac{a}{\phi}(O_2 + 3.762N_2) \rightarrow b_1CO_2 + c_1H_2O + d_1O_2 + 3.762\frac{a}{\phi}N_2, \tag{2}$$

and as more fuel is added,

2. To create CO:

$$C_xH_y + \frac{a}{\phi}(O_2 + 3.762N_2) \rightarrow b_2CO_2 + c_2H_2O + e_2CO + 3.762\frac{a}{\phi}N_2, \tag{3}$$

and then as even more fuel is added,

3. To create carbon soot, $C_{(S)}$:

$$C_xH_y + \frac{a}{\phi}(O_2 + 3.762N_2) \rightarrow c_3H_2O + e_3CO + f_3C_{(S)} + 3.762\frac{a}{\phi}N_2, \tag{4}$$

and thereafter, as the fuel becomes in a large excess, the combustion reaction is extinguished, and

4. The unburned fuel coexists with reacted substance, the latter consisting of water vapour, H_2O, and carbon soot, $C_{(S)}$:

$$C_xH_y + \frac{a}{\phi}(O_2 + 3.762N_2) \rightarrow c_4H_2O + f_4C_{(S)} + g_4C_xH_y + 3.762\frac{a}{\phi}N_2. \tag{5}$$

Here, $a = x + \frac{y}{4}$; ϕ is the equivalence ratio, i.e. (actual fuel-to-air ratio)/(stoichiometric fuel-to-air ratio); and a, b, c, d, e, f, g are molar coefficients.

In above and throughout the text below it is also generally assumed that atmospheric air contains 23.3% of oxygen and 76.7% of nitrogen, i.e. 3.762 molecules of N_2 per one molecule of O_2.

In terms of chemical elements involved, the above oxidation stages are represented by four-zone discretization of free oxygen element, (O)-element, space as follows:

1. lean-mixture zone, in which (O)-element mass fraction exceeds its stoichiometric limiting value;
2. intermediate, in which (O)-element mass fraction lies in between the stoichiometric and intermediate limits;
3. sooting, in which (O)-element mass fraction lies in between the intermediate and soot limits; and
4. fuel-rich zone, where (O)-element mass fraction is below the soot limit.

3.2. Flame limits

From discrete chemical reactions, the equations for the mass fractions of elements in each zone are first obtained. The stoichiometric limit is characterized by the absence of fuel, molecular oxygen, carbon monoxide and carbon soot; the limiting value of oxygen element, $m_{(O)st}$, is then readily calculated as

$$m_{(O)st} = \frac{32}{12} m_{(C)} + \frac{16}{2} m_{(H)}. \tag{6}$$

The intermediate limit, $m_{(O)in}$, is obtained on the grounds that no fuel exists, and neither molecular oxygen, nor carbon dioxide, and never carbon soot are present in the products.

$$m_{(O)in} = \frac{16}{12} m_{(C)} + \frac{16}{2} m_{(H)}. \tag{7}$$

It is believed reasonable to assume that at the soot limit, $m_{(O)S}$, only nitrogen, water vapour, and carbon soot can be found in the mixture so that

$$m_{(O)S} = \frac{16}{2} m_{(H)}. \tag{8}$$

The above limiting requirements are expressed as algebraic relations, and can be viewed as problem specific parameters of grid adaptation in (O)-element variable space.

3.3. Product compositions

If the mass fraction of (O)-element becomes larger than its stoichiometric limit, $m_{(O)} \geqslant m_{(O)st}$, there is an excess of oxygen. The fast chemistry implies that neither of combustible components (no fuel, no carbon monoxide, no soot) can exist, i.e. $m_{fu} = 0$, $m_{CO} = 0$ and $m_{C_{(S)}} = 0$. At this point, the element mass fraction expressions are reduced to

$$m_{(O)} = m_{O_2} + \frac{32}{44} m_{CO_2} + \frac{16}{18} m_{H_2O}, \tag{9}$$

$$m_{(C)} = \frac{12}{44} m_{CO_2}, \tag{10}$$

$$m_{(H)} = \frac{2}{18} m_{H_2O}, \tag{11}$$

which is a set of three equations in three unknowns m_{O_2}, m_{CO_2}, and m_{H_2O}.

The similar reductions can be performed for each of the three other zones guided by the product composition defined by discrete chemical equations (2)–(5) and fast chemistry assumptions. Thus, in either zone there will be the closed set of three linear equations for three component mass fractions. The exact solutions are easy to obtain, from which the unknown component mass fractions can readily be found.

The actual algebra and related manipulations have to be left to the reader. The resulting algebraic equations for each reaction zone are presented below in terms of element mass fractions:

1. Lean-mixture zone ($m_{(O)st} \leqslant m_{(O)}$):

$$m_{fu} = m_{CO} = m_{C_{(S)}} = 0.0, \tag{12}$$

$$m_{H_2O} = \frac{18}{2} m_{(H)}, \tag{13}$$

$$m_{O_2} = m_{(O)} - m_{(O)st}, \tag{14}$$

$$m_{CO_2} = \frac{44}{12} m_{(C)}. \tag{15}$$

2. Intermediate zone ($m_{(O)in} \leqslant m_{(O)} \leqslant m_{(O)st}$):

$$m_{O_2} = m_{fu} = m_{C_{(S)}} = 0.0, \tag{16}$$

$$m_{H_2O} = \frac{18}{2} m_{(H)}, \tag{17}$$

$$m_{CO} = \frac{28}{16} (m_{(O)st} - m_{(O)}), \tag{18}$$

$$m_{CO_2} = \frac{44}{12} \left(m_{(C)} - \frac{12}{28} m_{CO} \right). \tag{19}$$

3. Sooting zone ($m_{(O)S} \leqslant m_{(O)} \leqslant m_{(O)in}$):

$$m_{O_2} = m_{fu} = m_{CO_2} = 0.0, \tag{20}$$

$$m_{H_2O} = \frac{18}{2} m_{(H)}, \tag{21}$$

$$m_{CO} = \frac{28}{16} (m_{(O)} - m_{(O)S}), \tag{22}$$

$$m_{C_{(S)}} = m_C - \frac{12}{16} (m_{(O)} - m_{(O)S}). \tag{23}$$

4. Fuel-rich zone ($m_{(O)} \leqslant m_{(O)S}$):

$$m_{O_2} = m_{CO_2} = m_{CO} = 0.0, \tag{24}$$

$$m_{H_2O} = \frac{18}{16} m_{(O)}, \tag{25}$$

$$m_{fu} = \frac{12x + y}{y} \left(m_{(H)} - \frac{2}{16} m_{(O)} \right), \tag{26}$$

$$m_{C_{(S)}} = m_{(C)} + \frac{12x}{y} \left(\frac{2}{16} m_{(O)} - m_{(H)} \right). \tag{27}$$

For any zone:

$$m_{N_2} = m_{(N)} = 1 - m_{fu} - m_{O_2} - m_{CO_2} - m_{H_2O} - m_{CO} - m_{C_{(S)}}. \tag{28}$$

Eqs. (12)–(27) are defined here as DRM, discrete reaction model, formulations. It is the recommended method for computing the composition of sooting flames, which is referred to below as the "present method".

3.4. Mixture-fraction-based formulations

The coefficients of discrete chemical equations (2)–(5) are easily expanded by applying the atomic conservations as shown in Appendix A. The resulting equations can be used to convert the present method into the expressions based on widely used definition of mixture fraction. The main details are given below.

Let us define the mixture fraction, f, as the local fuel mass fraction, where "fuel" means the entire fuel stream. The mixture fraction is allowed to vary between 0 and 1, and is connected with common measures of combustion systems as follows:

$$f = \frac{\phi}{\phi + \chi}. \tag{29}$$

Here, χ is the stoichiometric air-to-fuel ratio on a mass basis, which is calculated as

$$\chi = (32 + 28 \cdot 3.762) \frac{a}{12x + y}. \tag{30}$$

The following is the mixture fraction at the stoichiometric limit where complete combustion takes place

$$f_{st} = \frac{1}{1 + \chi}. \tag{31}$$

The mixture fraction at rich limit is as follows:

$$f_{in} = \frac{1}{1 + \chi \frac{2x+y}{4x+y}}. \tag{32}$$

The following is readily obtained for the soot limit of mixture fraction:

$$f_s = \frac{1}{1+\chi\frac{y}{4x+y}}. \tag{33}$$

Then through the calculation of limiting values for inert nitrogen mass fractions, and corresponding mass fraction of total products, the individual mass fractions for all product components at the mixture fraction limits are computed. The local mass fraction formulations are finally derived, in a piecewise linear manner, from mixture fraction values as the following expressions for the sooting zone exemplify:

$$m_{O_2} = m_{fu} = m_{CO_2} = 0, \tag{34}$$

$$m_{CO} = \frac{28x}{28x+\frac{18}{2}y}[1-0.767(1-f_{in})]\left(1-\frac{f-f_{in}}{f_s-f_{in}}\right), \tag{35}$$

$$m_{C_{(S)}} = \frac{12x}{12x+\frac{18}{2}y}[1-0.767(1-f_s)]\frac{f-f_{in}}{f_s-f_{in}}, \tag{36}$$

$$m_{H_2O} = \frac{\frac{18}{2}y}{44x+\frac{18}{2}y}[1-0.767(1-f_{st})]\frac{f}{f_{st}}, \tag{37}$$

$$m_{N_2} = m_{(N)} = 1 - m_{fu} - m_{O_2} - m_{CO_2} - m_{H_2O} - m_{CO} - m_{C_{(S)}}. \tag{38}$$

Eqs. (34)–(37) and similar relations for all other reaction zones are found in Appendix B. They can all be summed up graphically as illustrated in Fig. 1.

This technique is referred to below simply as a "mixture fraction method", and may only be applied to the situations within the limitations of mixture-fraction-based methods [1].

4. Implementation

The present treatment of the stream of sooting mixture is assumed to be similar to single-phase flow, i.e. the flow is considered homogeneous, so that no slip velocity exists between soot particles and the gas components, and there is no influence of the soot parcels on the turbulence structure.

Based on that the set of time-averaged conservation equations for flow mass, its momentum and energy, chemical elements and turbulence variables of two-equation $K-\varepsilon$ model of turbulence, all take the general form:

$$\frac{\partial(\rho\varphi)}{\partial t} + div(\rho\vec{V}\varphi) = div(\Gamma_\varphi grad\varphi) + S_\varphi, \tag{39}$$

where $\rho, \vec{V}, \Gamma_\varphi$, and S_φ are density, velocity vector, effective exchange coefficient of φ, and source rate, respectively. The sources and exchange coefficients for velocities and turbulence quantities have been often discussed elsewhere, and are not repeated here. The thermal radiation contributes to the source term for mixture enthalpy.The DRM analysis can readily be used to estimate the mixture composition on cell-by-cell basis. The following approach is suggested:

(i) The element mass fractions are calculated from their own conservation equations.
(ii) For each cell the flame limits are checked, and relevant reaction zone identified via (6)–(8).
(iii) The appropriate expression of (12)–(27) is used to compute the mass fraction of mixture component.
(iv) Repeat (iii) for all participating mixture species.

If the mixture fraction formulations seem to be preferable the distributions of f are calculated from its source-free conservation equation. Then the equations of mixture fraction method should be used at (ii) and (iii). In some cases direct algebraic conversion of mixture fraction distribution into element mass fractions can be economically employed.

In typical flame system, the temperatures can range to over 2000 K. Thus, radiation effects must be included. The extended P-1 type radiation model used here entails solution of the transport equation for the incident radiation [1]. However, its exchange coefficient has been re-formulated to include the "stopping distance" affected by bounding walls as follows:

$$\Gamma_R = \frac{1}{3(a+s+1/W_{gap})-C_g s}, \tag{40}$$

where a is the absorption coefficient; s is the scattering coefficient; W_{gap} is the distance between adjacent walls, and C_g is the symmetry factor of a scattering phase function.

The inclusion of $1/W_{gap}$ in the exchange coefficient expression is the only significant feature of the current radiation model. It has its origin in IMMERSOL model of PHOENICS [7] and allows the coefficient to remain finite even for very optically thin gases when a and s are infinitely small. In physical terms, whereas $1/(a+s)$ represents the mean free path (or average ray-stopping distance) associated with absorption and scattering, W_{gap} represents the distance between the bounding walls of the space. The latter is thought of as the "stopping distance" effected by those walls and allows the radiative exchange coefficient to vary realistically from place to place in complex congested spaces even if the radiative properties of the medium remain constant.

The solution of the following Poisson equation for distance function L [7] allows the calculation of W_{gap} to be completed with relative easy even for spaces cluttered with the solids:

$$div(grad\ L) = 0 \tag{41}$$

with $L = 0$ at the solid walls. The solution is then algebraically converted into easy-to-compute relation:

$$W_{gap} = 2\sqrt{|gradL|^2 + 2L}. \tag{42}$$

Gas properties are obtained through local mixing calculations. The specific heat of individual components is assumed to depend linearly on the local temperature. The relation constants were optimized so as to produce the best possible fit for the individual specific heats, over the typical range of temperature; the reference values being those reported in the literature.

Gas mixture absorption coefficient is represented as a linear composition of absorption coefficients for optically participating species and their partial pressures. The total absorption coefficient of a sooting gas mixture is computed as the sum of the absorption coefficients for pure gas mixture and soot. The latter is computed via soot concentration and local temperature.

The conventional boundary conditions are used for wall friction (velocities) and turbulence quantities. For the radiation equations

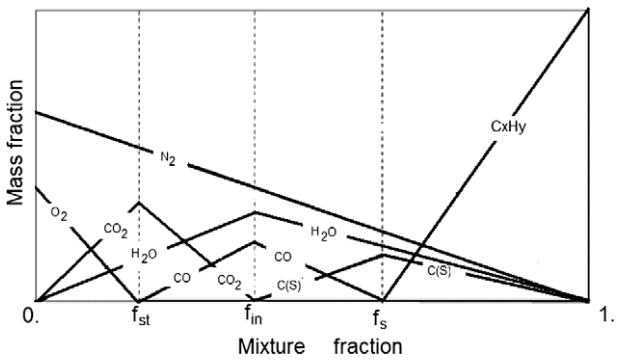

Fig. 1. Mixing and fast reaction between fuel ($f = 1$), and oxidant ($f = 0$) streams. (Not to scale.)

boundary sources are derived from the near-wall heat balance. The sources for incident radiation at the inlets and outlets are computed in the manner similar to the walls.

The set of governing equations closed by the composition equations, with the boundary conditions, and the radiation transport model equation– all were solved by commercially available PHOENICS code [7].

5. Validation example: performance of carbon black furnace

5.1. Problem statement

In the furnace black process, schematically shown in Fig. 2, fuel (usually natural gas) is burnt under fuel lean conditions in the primary stage. In a secondary stage a feedstock, usually oil is injected through an atomizer into the hot exhaust from the primary stage. After the reaction mixture is quenched with water and cooled in heat exchangers, the carbon black is collected from the product (tail) gas using a filter system. The stream chart shown in Fig. 3 illustrates the operational conditions used as the model inputs.

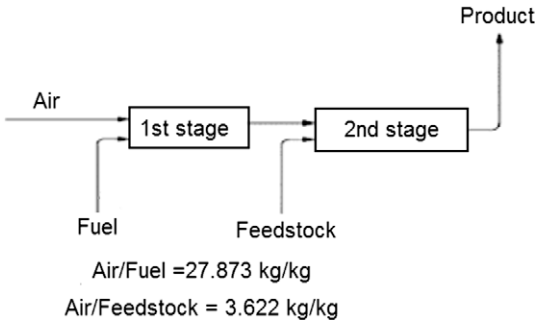

Fig. 3. Furnace stream chart.

Table 1
Predicted results compared to measured values (actual) in a furnace.

Variable	Predicted by detailed method [9]	Predicted by present method	Actual
Exit soot mass fraction (kg/kg)	0.086	0.1683	0.127
Yield (kg carbon/kg feedstock)	0.407	0.7983	0.605

5.2. Discussion of results

In the case study, the field distributions of gas composition are predicted from which the averaged exit values of the carbon soot mass fraction and yield (kg of carbon soot per kg of feedstock) are computed. The simulation tests the model against industrial data of Philips Petroleum Company as reported by Lockwood and van Niekerk [8]. Only overall product values such as soot mass fraction and yield were available for comparison. The results for the test simulations are presented in Table 1.

The results of Table 1 suggest that the present method is in agreement with the experimental observations. The soot mass fraction and yield are over predicted by about 30%. Indeed it can be expected that the present prediction will give larger values of soot mass fractions, because the reaction is presumed to be infinitely fast.

The validation exercises also suggest that results of the detailed approach taken from [9], even augmented there by experimental mixing rate, is in no better agreement with experiment; for the detailed calculations under predict the soot contents by about the same percentage. This can be attributed to the lack of universality in the number of specific assumptions made in the formulation of the detailed model. In addition over-simplified nature of the flow model used in [9] to represent reactor as an assembly of perfect and partially stirred sections was almost certainly far from adequate.

The application of the mixture fraction approach appears to be possible only for the simulation of the primary stage. There, the mixture is highly fuel lean, and the inlet streams are made up entirely from fuel and oxidizer; the situation that is not to be found in secondary zone. In the latter one of the inlet streams is formed by the first stage flue gas and feedstock composition is different from primary fuel.

The effects of feedstock on the composition of the product gas were investigated. The performance of the furnace with both diesel fuel and heptanes as a feedstock is found to be far from being acceptable; for almost the same amount of feedstock as the carbon of soot produced is thrown away with exhaust gases. Even highly sooting toluene cannot compete with aromatic oil in terms of feedstock consumption; for it is also unable to react completely under given operating conditions. The aromatic oil as a feedstock solves the problem of reaction incompleteness. Variation of feedstock type has also revealed that the present model predicts the decrease in propensity to soot with the level of hydrocarbon saturation. Aliphatic feedstock such as methane and ethane were much less sooting than aromatics.

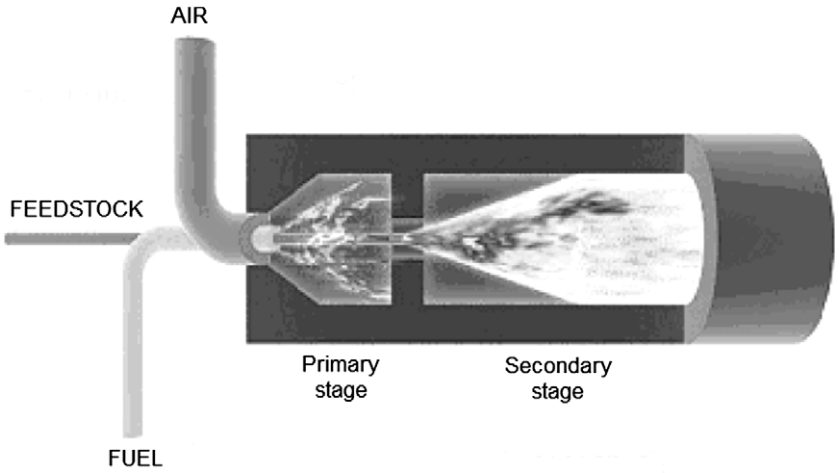

Fig. 2. Computational schematic of a carbon black furnace.

The effects of varying equivalence ratio in the primary stage were also studied. It was predicted that the yield increases in linear manner with the increase in primary equivalence ratio. For the fuel-rich state of the base product mixture a small increase in the oxygen contents of air increases the yield, but a large increase in oxygen fraction significantly decreased soot tendency.

All these trends are in accord with existing technological experience [10]. The similar observations have also been reported in the simulations performed elsewhere [8,9]. Given the number of assumptions made in the formulation of the present model and in the representation of the furnace, and also the fact that no changes have been made to any of the reaction modelling equations, the present model predictions look fair and versatile and may be regarded as satisfactory for engineering purposes.

In contrast, the simplified analysis could not be uniformly applicable to the reactor operating conditions; for the user should always perform sample calculations to obtain trial values of conversion factors prior to using the simplified methods. For many situations the mixture fraction approach will suffice; but this will not be the case here as the streams have different compositions. The present analysis does generate meaningful results for non-similar inlet streams, and for all specified states of product mixture: lean, intermediate, sooting, and rich. It is therefore recommended.

While it is possible to construct more complex problems, this simple example has served to validate and illustrate the typical performance of the present model.

6. Some engineering applications

6.1. Flame in a cylindrical furnace

As a further validation, an application of DRM to the development of the turbulent diffusion flame in a cylindrical furnace with a thermal input of 400 kW [11] is considered. The natural gas and air are admitted through two coaxial jets with inlet diameters of 60 and 100 mm into the combustion chamber the diameter and length of which are 0.5 and 1.7 m, respectively. The composition of natural gas is taken as 90% methane and 10% nitrogen. A computational grid with 55 cells in the axial and 45 cells in the radial direction was employed. Fig. 4 shows the predicted temperature distribution in the combustion chamber. Shown in Fig. 5 are the longitudinal distributions of fuel and water vapour.

In general, the agreement between predictions and experimental observations is seen to be good for the products of the complete combustion available for comparison.

6.2. Lead-smelting furnace

The furnace under consideration is usually equipped with two natural gas fired burners in one end wall and a rectangular exhaust port in the other end wall. The roof is arched (refractory) and the burners are slightly inclined toward the bath.

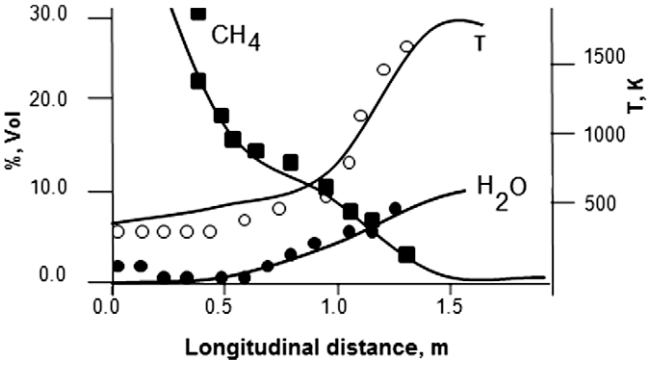

Fig. 5. Predictions (lines) vs. experiments.

Fig. 6 illustrates the furnace geometry. The apertures for burners are seen at the left end wall; air and fuel gas are admitted through separate circular slots. A rectangular exhaust port is also shown at the right end wall. The inlet conditions are set in the model as the mass flow rate at the firing rates of 1.5 GJ/h per burner. The excess air is provided at 5%.

Illustrated on Fig. 7 is the distribution of the temperatures and velocity vectors at the burner plane. Inspection of the Fig. 7 and other resulting fields reveal expected trends resulting from conflicting effects of forced inflow (directed downwards) and buoyancy forces working in opposite directions. In fact, the simulated flow pattern reflects the fact that the flow in the vicinity of the burners is going down as a result of inclined inlet momentum, and that the hot combustion gases go up in the regions where the buoyancy dominates. The test calculations have also showed that the predicted adiabatic flame temperature agrees well (within 3%) with the theoretical value for simulated conditions.

As soot effectively changes radiative heat transfer from the combustion environment to all surfaces, heat fluxes to both refractory and melted lead surfaces are under-predicted when soot formation is not taken into account. It gives the refractory and lead surface temperatures that are on average more than 70 °C too low. The temperature peak that is observed in practice is only accurately predicted when soot formation is included in the combustion model.

The amount of soot being formed depends strongly on the type of the fuel. DRM predicts that natural gas, methane and propane/butane mixtures give relatively low soot concentration compared to fuel oil. The predictions show that using fuel oil, approximated as $C_{21}H_{44}$, the higher flux and more uniform distribution of the heat to the melted lead surface can be achieved, leading to the significant decrease in average exhaust gas temperatures.

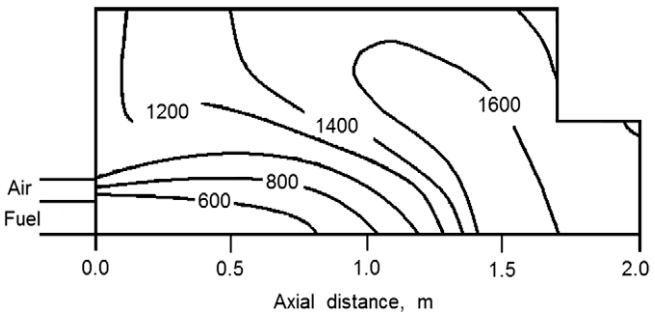

Fig. 4. Predicted temperature distribution in K.

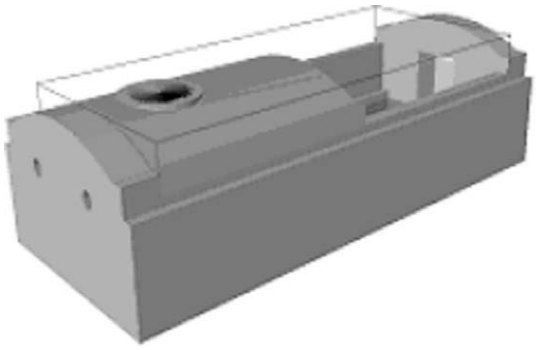

Fig. 6. Geometry of a smelting furnace.

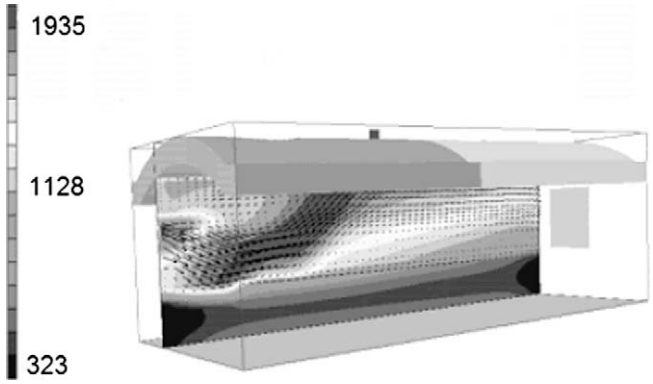

Fig. 7. Distribution of the temperatures (K) and velocity vectors at the burner plane.

Taken together the predicted results have shown that practical simulations and quantitative realistic calculations of heat and mass transfer in three-dimensional furnaces can be performed with the aid of the model developed. The general trends are correctly predicted. This indicates that the model can be applied as a design tool to test the effects of alternative configurations and/or the operational conditions of the furnace.

6.3. Thermal radiation in a compartment fire

The case simulated corresponds to the experiment conducted by Steckler et al. [12] who investigated fire induced flows in a compartment of 2.8 m wide, 2.8 m long, and 2.18 m high. Three distinct test cases were examined for demonstration and validation purposes. Both refer to the above room geometry; and they differ with respect to the account of radiative heat transfer and participating soot.

The present calculations have proved that neglecting the effects of soot on radiative heat transfer generally lead to over-prediction of the temperatures. When soot absorption of radiation is appropriately accounted for the simulation results and measurements compare reasonably well.

Shown in Fig. 8 are the distributions of the temperature at the middle of the doorway. The decrease in temperature when radiation and soot are both included is clearly evident.

7. General discussion

The DRM, as developed, represents the global chemistry of hydrocarbon oxidation by a finite number of chemical reaction each associated with certain range of O-element mass fraction. The element-based formulations of present DRM are, by and large, well adapted to different uses arising from industrial combustion applications. The author's position is that the present element-based and linear mixture-fraction-based formulations should be entirely equivalent, provided that the limitations of the latter are not compromised.

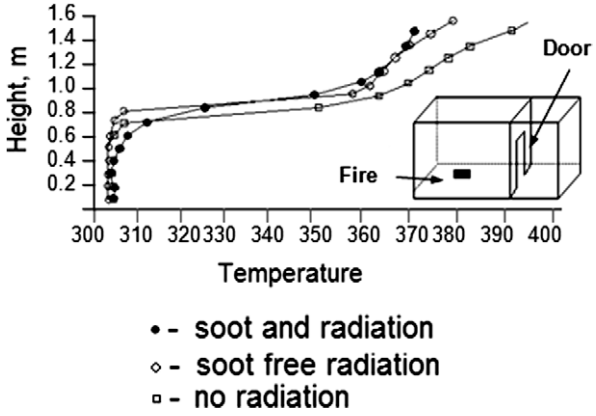

Fig. 8. Vertical temperature (K) profile at the middle of the doorway.

It can be shown that the same line of arguments that resulted in the DRM formulations produces the well known relationships of simple chemical reaction scheme, SCRS [13], when the products of hydrocarbon oxidation are restricted to the main compounds, namely CO_2 and H_2O. The present approach therefore is not in any conflict with the more usual one, but rather generalizes it, making calculations possible in complex cases where the mixture fraction method would be too clumsy (if of any use at all).

In this paper, one example of direct model validation for the prediction of product composition produced in a black carbon furnace fuelled and fed by different hydrocarbons was given, followed by a few further engineering applications. The predictions have demonstrated a fair agreement to the experimental observations. This was achieved without making any ad hoc adjustments to the original concept of the present approach; the theory is sufficient to adequately describe a variety of possible scenarios.

It was also demonstrated that the present method may readily be used in the calculation procedures involving thermal effects of heat releases and radiation. The DRM formulations being of algebraic nature are easy to import into single- or multi-phase solvers of available CFD software. The model framework is seen to be flexible enough to readily accommodate the modelling techniques for the turbulence–chemistry interactions, such as presumed PDF [2,14], or multi-fluid population balance [15].

It might be argued, however, that there are the situations for which the present analysis does not hold. In those circumstances there might be no other recourse than to solve an eddy dissipation type of soot formation model [16], or two-step Tesner model [17], or even a joint PDF transport equation [2] to combine the detailed soot modelling with a stochastic mixing.

There are also a number of other important factors to consider when analyzing composition of sooting flames. For example, the present approach has a potential to (and must) be extended if larger number of product species are to be taken into account. Non-equilibrium effects may be important, and soot particle size distributions should be used to describe the kinetics of soot formation. While the importance of turbulence–chemistry interaction, finite rates of reactions, and the stochastic nature of soot particle formation, agglomeration, and oxidation is not to be understated, there is clearly a range of applications, where the present method would give reasonable estimate of sooting flame composition.

8. Conclusions

An analysis based on the well-established concept of chemical element conservation was adapted to the novel reaction model developed to predict the composition of sooting flames. The model is designed as a discrete reaction set for multi-stage approximation of hydrocarbon oxidation taking place in a seven-species mixture of reactants and products obtained on the grounds of fast reaction chemistry.

The discrete reaction model has been shown to be an effective and rather simple method for prediction of sooting flame compositions. It was demonstrated that the predictions made by the present approach are in fair agreement with measured data without making any adjustments to the soot-forming reactions. The trends predicted are also correct. An approach based on mixture fraction

provides identical results, although it does not appear to offer any major advantages over the present analysis, which is working well beyond the limitations of the former.

The model developed has the advantage of being in a form fully compatible with methods widely used in CFD practice, and, therefore, has a potential to supplant or complement the latter in the computational analysis of combustion phenomena in practical engineering equipment.

Acknowledgements

Dr. M.R. Malin of CHAM Ltd. contributed some useful discussion about the DRM in the early stages of the project. Ms. Natalia Joubrina provided technical support. The support of ACFDA Inc. of Canada is acknowledged with gratitude.

Appendix A. Chemical equations for discrete reactions of sooting combustion

The chemical equations (2)–(5) are readily expanded by atomic balances. In the full form they are as follows:

1. The lean-mixture zone ($0 < \phi \leqslant \phi_{st}$)

$$C_xH_y + \frac{a}{\phi}(O_2 + 3.762N_2) \rightarrow xCO_2 + \frac{y}{2}H_2O + a\frac{1-\phi}{\phi}O_2 + 3.762\frac{a}{\phi}N_2. \tag{A.1}$$

2. The intermediate zone ($\phi_{st} < \phi \leqslant \phi_{in}$)

$$C_xH_y + \frac{a}{\phi}(O_2 + 3.762N_2) \rightarrow \left(2a\frac{1-\phi}{\phi} + x\right)CO_2 + \frac{y}{2}H_2O + 2a\frac{\phi-1}{\phi}CO + 3.762\frac{a}{\phi}N_2. \tag{A.2}$$

3. The sooting zone ($\phi_{in} < \phi \leqslant \phi_s$)

$$C_xH_y + \frac{a}{\phi}(O_2 + 3.762N_2) \rightarrow \frac{y}{2}H_2O + 2\left(a\frac{1-\phi}{\phi} + x\right)CO + \left(2a\frac{\phi-1}{\phi} - x\right)C_{(S)} + 3.762\frac{a}{\phi}N_2. \tag{A.3}$$

4. The fuel-rich zone ($\phi > \phi_s$)

$$C_xH_y + \frac{a}{\phi}(O_2 + 3.762N_2) \rightarrow \frac{2a}{\phi}H_2O + \frac{4ax}{\phi y}C_{(S)} + \left(1 - \frac{4a}{\phi y}\right)C_xH_y + 3.762\frac{a}{\phi}N_2. \tag{A.4}$$

Here, $a = x + y/4$.

The limiting equivalence ratios are readily obtained, as follows:

$$\phi_{st} = 1, \tag{A.5}$$

$$\phi_{in} = \frac{4x+y}{2x+y}, \tag{A.6}$$

$$\phi_s = 1 + 4\frac{x}{y}. \tag{A.7}$$

The chemical equations at the flame limits are the special cases of discrete reactions (A.1)–(A.4) under the limiting equivalence ratios (A.5)–(A.7):

Stoichiometrical limit ($\phi = 1$):

$$C_xH_y + \left(x + \frac{y}{4}\right)(O_2 + 3.762N_2) \rightarrow \frac{y}{2}H_2O + xCO_2 + 3.762\left(x + \frac{y}{4}\right)N_2. \tag{A.8}$$

Rich limit ($\phi = \phi_{in}$):

$$C_xH_y + \left(\frac{x}{2} + \frac{y}{4}\right)(O_2 + 3.762N_2) \rightarrow \frac{y}{2}H_2O + xCO + 3.762\left(\frac{x}{2} + \frac{y}{4}\right)N_2. \tag{A.9}$$

Soot limit ($\phi = \phi_s$):

$$C_xH_y + \frac{y}{4}(O_2 + 3.762N_2) \rightarrow \frac{y}{2}H_2O + xC_{(S)} + 3.762\frac{y}{4}N_2. \tag{A.10}$$

Appendix B. Mixture fraction formulations for sooting flames

Given the mixture fraction the values for the species mass fractions after combustion of undiluted hydrocarbon fuel in the presence of oxygen from atmospheric air are obtained from

- if $0 \leqslant f \leqslant f_{st}$:

$$m_{fu} = m_{CO} = m_{C_{(S)}} = 0, \tag{B.1}$$

$$m_{O_2} = 0.233\left(1 - \frac{f}{f_{st}}\right), \tag{B.2}$$

$$m_{H_2O} = \frac{\frac{18}{2}y}{44x + \frac{18}{2}y}[1 - 0.767(1 - f_{st})]\frac{f}{f_{st}}, \tag{B.3}$$

$$m_{CO_2} = \frac{44x}{44x + \frac{18}{2}y}[1 - 0.767(1 - f_{st})]\frac{f}{f_{st}}, \tag{B.4}$$

- if $f_{st} \leqslant f \leqslant f_{in}$:

$$m_{O_2} = m_{fu} = m_{C_{(S)}} = 0, \tag{B.5}$$

$$m_{H_2O} = \frac{\frac{18}{2}y}{44x + \frac{18}{2}y}[1 - 0.767(1 - f_{st})]\frac{f}{f_{st}}, \tag{B.6}$$

$$m_{CO} = \frac{28x}{28x + \frac{18}{2}y}[1 - 0.767(1 - f_{in})]\frac{f - f_{st}}{f_{in} - f_{st}}, \tag{B.7}$$

$$m_{CO_2} = \frac{44x}{44x + \frac{18}{2}y}[1 - 0.767(1 - f_{st})]\left(1 - \frac{f - f_{st}}{f_{in} - f_{st}}\right), \tag{B.8}$$

- if $f_{in} \leqslant f \leqslant f_s$:

$$m_{O_2} = m_{fu} = m_{CO_2} = 0, \tag{B.9}$$

$$m_{CO} = \frac{28x}{28x + \frac{18}{2}y}[1 - 0.767(1 - f_{in})]\left(1 - \frac{f - f_{in}}{f_s - f_{in}}\right), \tag{B.10}$$

$$m_{C_{(S)}} = \frac{12x}{12x + \frac{18}{2}y}[1 - 0.767(1 - f_s)]\frac{f - f_{in}}{f_s - f_{in}}, \tag{B.11}$$

$$m_{H_2O} = \frac{\frac{18}{2}y}{44x + \frac{18}{2}y}[1 - 0.767(1 - f_{st})]\frac{f}{f_{st}}, \tag{B.12}$$

- if $f \geqslant f_s$:

$$m_{O_2} = m_{CO_2} = m_{CO} = 0, \tag{B.13}$$

$$m_{H_2O} = \frac{\frac{18}{2}y}{12x + \frac{18}{2}y}[1 - 0.767(1 - f_s)]\left(1 - \frac{f - f_s}{1 - f_s}\right), \tag{B.14}$$

$$m_{C_{(S)}} = \frac{12x}{44x + \frac{18}{2}y}[1 - 0.767(1 - f_s)]\left(1 - \frac{f - f_s}{1 - f_s}\right), \tag{B.15}$$

$$m_{fu} = \frac{f - f_s}{1 - f_s}, \tag{B.16}$$

- for any f,

$$m_{N_2} = 1 - m_{fu} - m_{O_2} - m_{CO_2} - m_{H_2O} - m_{CO} - m_{C_{(S)}}. \tag{B.17}$$

References

[1] K. Kuo, Principles of Combustion, third ed., John Wiley and Sons, New York, 2004. pp. 760.

[2] R.P. Lindstedt, S.A. Louloudi, Joint-scalar transported PDF modelling of soot formation and oxidation, Proc. Combust. Inst. 30 (2005) 775–783.
[3] V. Novozhilov, H. Koseki, Computational fluid dynamics prediction of self-sustained pool fire combustion, J. Inst. Eng. 1 (5) (2004) 69–81.
[4] J.E. Floyd, K.B. McGrattan, S. Hostikka, H.R. Baum, CFD fire simulation using mixture fraction combustion and finite volume radiative heat transfer, J. Fire Protect. Eng. 13 (2003) 11–34.
[5] D.B. Spalding, A standard formulation of the steady convective mass transfer problem, Int. J. Heat Mass Transfer 1 (1960) 192–207.
[6] D.B. Spalding, Convective Mass Transfer; an Introduction, Edward Arnold, London, 1963. pp. 384.
[7] PHOENICS 3.6.1, CHAM Ltd., 2007.
[8] F. Lockwood, J. Van Niekerk, Parametric study of carbon black oil furnace, Combust. Flame 103 (1995) 76–90.
[9] M. Balthasar, F. Mauss, A. Knobel, M. Kraft, Detailed modeling of soot formation in a partially stirred flow reactor, Combust. Flame 128 (2002) 395–409.
[10] E.M. Dannenberg, L. Paquin, H. Gwinell, Carbon black, in: Encyclopedia of Chemical Technology, third ed., John Wiley and Sons, New York, vol. 4, 1978, pp. 631–666.
[11] D. Garreton, O. Simonin, First Aerodynamics of Steady State Combustion Chambers and Furnaces Workshop, EDF-DER, Chaton, 1994.
[12] K.D. Steckler, J.G. Quintiere, W.J. Rinkinen, Flow induced by Fire in a Compartment, NBSIR 82-520, U.S. Department of Commerce, National Bureau of Standards, 1982.
[13] D.B. Spalding, Combustion and Mass Transfer, Pergamon Press, London, 1979. pp. 410.
[14] W.P. Jones, J.H. Whitelaw, Calculation methods for reacting turbulent flows: a review, Combust. Flame 48 (1982) 1–26.
[15] S.V. Zhubrin, Multi-fluid model applied to a confined diffusion flame, PHOENICS J. Comput. Fluid Dyn. Appl. 12 (1) (1999) 79–94.
[16] B.F. Magnussen, B.H. Hjertager, On mathematical models of turbulent combustion with special emphasis on soot formation and combustion, in: Proceedings of 16th Symp. (Int'l.) on Combustion, The Combustion Institute, 1976, pp. 719–729.
[17] P.A. Tesner, T.D. Snegiriova, V.G. Knorre, Kinetics of dispersed carbon formation, Combust. Flame 17 (1971) 253–260.